

Wave-Particle Resonance in Magnetized Plasma

M. Sarfaty,¹ S. De Souza-Machado,² and F. Skiff²

¹Engineering Research Center, University of Wisconsin, Madison, Wisconsin 53706

²Institute for Plasma Research, University of Maryland, College Park, Maryland 20742-3511

(Received 19 June 1997)

We report the first observation of the wave-particle resonance line in a magnetized and weakly collisional plasma. The linear resonance satisfies the relation $\omega - n\Omega_{ci} = k_{\parallel}v_{\parallel}$ and has a width which is related to the wave-particle coherence time. Both the in-phase (real) and quadrature (imaginary) parts of the resonant response are directly determined by a phased-lock laser induced fluorescence diagnostic. The wave-particle coherence time obtained by fitting the resonance line shape to a one-dimensional Poisson-Fokker-Planck model does not agree with a simple model of ion collisionality. [S0031-9007(98)05751-2]

PACS numbers: 52.25.Dg, 52.35.-g, 52.70.Kz

Wave-particle resonance is a fundamental phenomenon in weakly collisional plasma. It provides the primary means for wave absorption and nonlinear interaction between waves. In models of infinite, uniform, and collisionless (Vlasov) plasma, the wave-particle resonance produces a singularity in the linear plasma response, for particle velocities which satisfy the resonance condition. The singularity problem is resolved in linear Vlasov models by proper treatment of initial and boundary conditions. In practice, the resonance must have a finite width which is determined by the finite interaction or coherence time between the particles and the wave, or by nonlinear effects. In the nonlinear regime, the resonance width is determined by the range of relative velocities that correspond to trapping in the wave potential. The linear wave-particle interaction theory ignores particle trapping, and fails if the coherence time becomes comparable to the period of particle oscillation in a wave trough. In addition, nearby resonances may have overlap of trapping widths [1] which may cause wave damping through particle-orbit chaos and reduction in wave-particle coherence. Resonant interaction is also at the core of a wide variety of plasma applications such as plasma heating, particle acceleration, and electromagnetic wave generators.

Despite this fundamental importance, no measurements of the linear wave-particle resonance line were reported. The first reason is that the measurement requires a sensitive and highly resolved velocity space diagnostic. A linear wave necessarily has a low amplitude, and the resonance line is a small feature on top of the perturbed distribution function. To be readily observed, the resonance line must be narrow compared to the thermal distribution. It is also true that the resonance line is not observed at every position in the wave field.

The second reason has to do with the strength of the wave-particle resonance. If the resonance occurs in the center of the velocity distribution function, then the wave fields are usually strongly damped, and do not extend uniformly over a significant plasma volume. Distribution functions measured under strong resonance condi-

tions show features which are a combination of wave and “ballistic” (Case–Van Kampen) response [2,3], i.e., free streaming of particles responding to a localized antenna. The phase information contained in the linear ion response for different ion velocities decays by destructive interference between these free-streaming modes. This strongly phase-mixed response can mask the resonance feature.

In our experiment, the wave-particle resonance is observed over a range of ion velocities defined by the resonance condition $\omega - n\Omega_{ci} = k_{\parallel}v_{\parallel}$, where ω is the wave angular frequency, $\Omega_{ci} = eB/Mc$ is the ion cyclotron frequency, v_{\parallel} and k_{\parallel} are the components of the ion velocity and wave number parallel to an externally applied magnetic field B . We observe $n = 1, 2$ resonances of electrostatic ion waves that propagate almost parallel to the B field. As the perpendicular wave number, and thus the electric field, is small, the wave damping and the excitation of ballistic perturbations are small enough that a clear resonance feature can be observed. The linearly perturbed ion velocity distribution is measured along the B field by a phase-locked laser induced fluorescence (LIF), using a single frequency scanning laser scheme [4].

Early observations of ion energy distributions in ion-acoustic waves were made with material probes using electrostatic analyzers [5–7]. The first LIF [8] observation of nonlocal ion heating by a current-driven instability was obtained from the ion velocity distribution. LIF observations of plasma dielectric motion [9–12] were determined by unfolding the information stored in the perturbed local ion velocity distribution. The ion response to electrostatic waves perpendicular to the B field was measured by a tunable pulsed dye laser time synchronized with the launched waves [9,10]. Wave-particle resonances were not observed in the linear ion response parallel to an ion-acoustic wave [11] due to strong phase mixing of ballistic perturbations over the long velocity distribution.

In this paper, wave-particle resonances are first observed in the linear ion response parallel to the B field. The resonance feature does not appear immediately at the wave launching antenna, but at a distance of about one

wavelength downstream of the antenna. This nonlocality is a central feature of the wave-particle resonance. Other related effects of the nonresonant part of the perturbed ion response are reported in Ref. [12].

The experiment is performed in an argon plasma column produced by radio frequency gas discharge and confined by an axial B field of 1 kG; see Fig. 1. The electrostatic ion-cyclotron waves are launched by a four ring antenna mounted on a computer controlled axial scanning carriage. The diameter and width of the rings are 5 and 1 cm, respectively, with a 3 cm spacing between the centers of adjacent rings. A biased wave transformer couples the wave generator to the antenna. The sinusoidal rf voltage pulse is applied with a phase difference of 180° between adjacent rings. The axial ring separation is set to roughly match a half wavelength of electrostatic ion-cyclotron waves in a frequency range of 30–100 kHz launched axially in argon plasma with electron density and temperature of $n_e \approx 2.5 \times 10^9 \text{ cm}^{-3}$ and $T_e \approx 2.8 \text{ eV}$. The ion temperature perpendicular and parallel to the B field is 0.05 and 0.065 eV, respectively.

The laser diagnostic, shown in Fig. 1, consists of a cw tunable dye laser (Rhodamine 6G) pumped by an argon ion laser. The ion velocity distribution is measured by scanning several GHz across the ion Doppler profile with a mode-locked narrow bandwidth ($<1 \text{ MHz}$) laser. The circularly polarized laser beam at 611.5 nm pumps the $\sigma = -1$ transitions of Ar II metastable state, $(3d')^2G_{9/2}$, into the $(4p')F_{7/2}$ level. The LIF at 461 nm into the $(4s')^2D_{5/2}$ state is used for diagnostics. An acousto-optic modulator temporally and spatially modulates the laser beam. The plasma ions are probed with the deflected part of the beam, while the undeflected part is used for beam diagnostics. The polarization of the beam is adjusted by a polarizing beam splitter, a half wave, and quarter wave plates that rotate and circularly polarize the beam. The laser beam power fluctuations are kept below 3%.

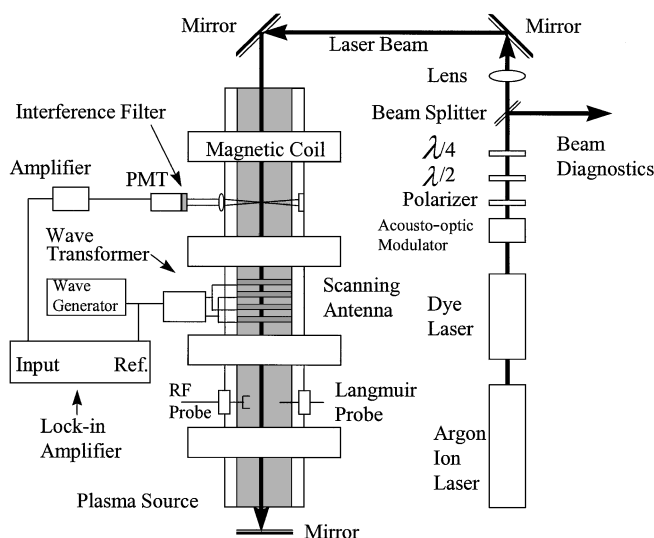


FIG. 1. Schematic description of the experimental setup.

The LIF is collected perpendicular to the laser beam downstream from the plasma source and the antenna. An optical 1 nm bandpass interference filter centered at the fluorescent line reduces the stray light into the photomultiplier tube (PMT). The amplified electrical signal of the PMT is sent to a lock-in amplifier and computer recorded. In the measurements of the coherent ion response to the waves, the laser beam is directed unmodulated into the plasma and the lock-in amplifier locks on the wave frequency. In the measurements of the ion velocity distribution, both in the presence and in the absence of waves, the lock-in amplifier locks on the laser modulation frequency. The ion velocity distribution, $f_0(v)$, and the linear ion response to the waves, $f_1(v)$, are obtained by scanning the laser frequency across the ion Doppler profile. The zero velocity of the ions in the lab frame is determined by the Lamb hole-burning effect using two counterpropagating laser beams. The accuracy of this method is $\approx 60 \text{ MHz}$ ($<10^{-4} \text{ nm}$) of laser frequency or ion velocity of $3.6 \times 10^3 \text{ cm/s}$.

The in-phase (real) and quadrature (imaginary) parts of the linear ion response to electrostatic waves are velocity resolved parallel to the B field. The normalized ion response 10 cm downstream of the antenna is plotted in velocity space in Fig. 2. A pronounced “bump” is evident in the profile of the 50 kHz wave at $v_{\parallel}/v_{\text{th}\parallel} \approx 1.25$. v_{\parallel} and $v_{\text{th}\parallel}$ are the components of the ion velocity and the thermal ion velocity parallel to the B field, respectively. Similarly, two bumps are observed in the profile of the 70 kHz wave at $v_{\parallel}/v_{\text{th}\parallel} \approx 2.7$ and ≈ -0.6 . Positive parallel velocity corresponds to a downstream flow of particles. These bumps are reproducible and have been observed over several experiments and under various scan ranges of laser frequency. Note that the higher signal fluctuations in the wings are due to lower photon counts than in the peaks. The resonance bumps are observed at ion velocities of higher photon counts.

The measured position of the wave-particle resonance in a wave frequency range of 30–80 kHz is shown in Fig. 3.

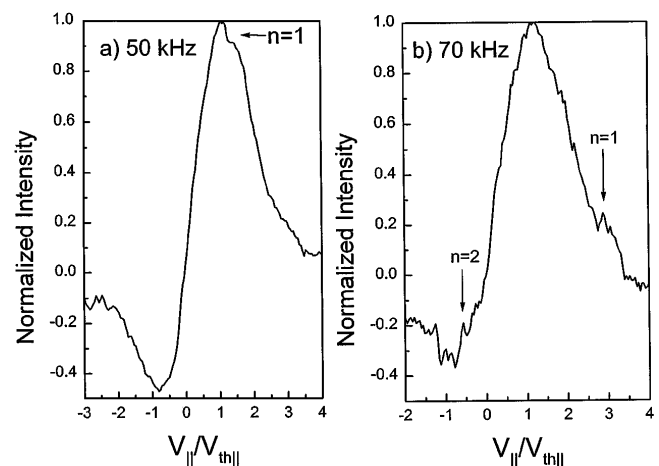


FIG. 2. The axial linear ion response to (a) 50 kHz and (b) 70 kHz wave frequencies.

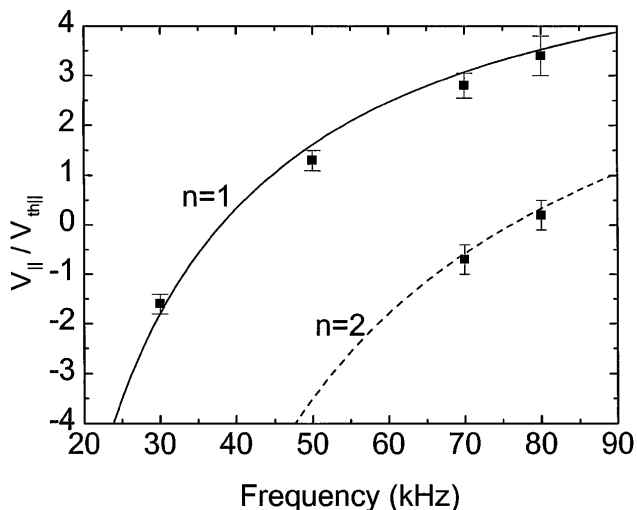


FIG. 3. The frequency dependent position of the wave-particle resonances for $n = 1$ (solid line) and $n = 2$ (dashed line) ion-cyclotron harmonics.

Wave frequencies outside this range resonate with ions in the tail of the ion velocity distribution resulting in poor signal-to-noise ratios. The lines trace the expected position of the $n = 1, 2$ ion-cyclotron wave-particle resonances. The uncertainty in the parallel ion velocity is estimated from the absolute determination of the laser frequency and the reproducibility of the wave-particle resonance position.

As the electrostatic waves launched by the antenna have a very small perpendicular wave vector [12] and $k_{\perp} \rho \ll 1$, the parallel wave vector is determined by $k_{\parallel} = \omega / c_s$; $c_s = (T_e / M)^{1/2}$. Substituting the wave dispersion relation into the wave particle resonance condition, $\omega - n\Omega_{ci} = k_{\parallel} v_{\parallel}$, provides a measure of the electron temperature from the observed position of the wave-particle resonance, $T_e = M[v_{\parallel} \omega / (\omega - n\Omega_{ci})]^2$. A very good agreement is found between the electron temperature measured by a Langmuir probe, by the wave dispersion relation [12], and that determined by the resonance position in velocity space.

The wave-particle coherence time is estimated by a model fit of the measured wave-particle resonance line shapes using a 1D Poisson-Fokker-Planck equation for the ions [13]. Ion collisions with electrons and neutrals are estimated to be 3 orders of magnitude smaller than ion-ion collisions, while charge exchange is about an order of magnitude smaller.

$$\frac{\partial f}{\partial t} + v \frac{\partial f}{\partial z} + \frac{e}{M} E(z, t) \frac{\partial f}{\partial v} = \nu \frac{\partial}{\partial v} \left(v f + v_{th}^2 \frac{\partial f}{\partial v} \right). \quad (1)$$

After linearization and Fourier-Laplace transforms [14], Eq. (1) is expressed by

$$\left\{ -i(\omega - kv) - \nu \left(1 + v \frac{\partial}{\partial v} + v_{th}^2 \frac{\partial^2}{\partial v^2} \right) \right\} f_1(\omega, k, v) = \frac{-e}{M} E(\omega, k) \frac{\partial f_0}{\partial v} + f_1(z = 0, \omega, v). \quad (2)$$

Under weak collisions the solution for the ion response in the range $|\omega - kv| = \nu$ assuming $\nu = \omega/k$ near the resonance, $\partial f_0 / \partial v = \text{constant}$, and $f_1(z = 0, k, v) = 0$ is given by

$$f_1(\omega, k, v) = \frac{-q}{M} E(\omega, k) \left(\frac{df_0}{dv} \right)_{v=\omega/k} \int_0^{\infty} d\tau e^{i\psi(v, \tau)}, \quad (3)$$

$$\psi(v, \tau) = \omega\tau - kv\tau - i\nu\tau - \frac{\nu\omega\tau^2}{2} + i\nu k^2 \frac{v_{th}^2 \tau^3}{3}. \quad (4)$$

$\psi(v, \tau = t - t_0)$ is the time dependent phase change of the wave due to interaction with the particles along their unperturbed orbits. The phase “memory” is attenuated by particle collisions or drag (third and fourth terms) and by particle velocity-space diffusion [14] (last term). The plasma parameters and wave frequencies in the experiment result in $k\lambda_{mfp} \approx 1-6$, which is marginal for the long mean free path approximation [14]. Introducing $\nu\tau = x$ in the integral of Eq. (3) denoted as D yields the following expression:

$$D = \int_0^{\infty} e^{i[(\omega - kv)/\nu]x} e^{-i(\omega/2\nu)x^2} e^x e^{-x_0(x/x_0)^3} dx, \quad (5)$$

$$x_0 = \sqrt{3} \nu / kv_{th} = \sqrt{3} \frac{1}{k\lambda_{mfp}}, \quad (6)$$

$$x = yx_0^{2/3} 3^{-1/3}, \quad \zeta = \frac{\omega - kv}{\nu} \left(\frac{x_0}{\sqrt{3}} \right)^{2/3} = \frac{\omega - kv}{kv_{th}} \left(\frac{kv_{th}}{\nu} \right)^{1/3}, \quad (7)$$

$$D(\zeta) = \int_0^{\infty} e^{i\zeta y} e^{-y^3/3} e^{-i(\omega/2\nu)(x_0/\sqrt{3})^{4/3} y^2} e^{y(x_0/\sqrt{3})^{2/3}} dy. \quad (8)$$

The real and imaginary parts of $D(\zeta)$ are numerically evaluated, for various values of the parameter x_0 . For $x_0 > 0.1$ the phase damping is dominated by the drag terms rather than the diffusion term. Also, the shape of $D(\zeta)$ varies with x_0 , which depends on the collision frequency and the wave and particle parameters. The profile of the linear ion response near the wave-particle resonance is given by

$$f_1(\omega, k, v, \nu) = \frac{-q}{M} E(\omega, k) \frac{\partial f_0}{\partial v} \tau_0 D(\zeta). \quad (9)$$

As the launched waves [12] have $k_{\perp} \rho \ll 1$ and $k_{\perp} / k_{\parallel} \leq 0.1$, a 1D model that includes the ion-cyclotron harmonics is used in the argument of the $D(\zeta) = [(\omega - kv - n\Omega) / \nu] (x_0 / \sqrt{3})^{2/3}$. The 1D model is used to qualitatively fit the measured ion response near the wave-particle resonance. The $D(\zeta)$ model was applied to each of the eight $\sigma = -1$ lines pumped by the circularly polarized laser. The convolved profile is compared to the experimental data, where the adjustable parameter is the plasma collision frequency. The best fit of the real and imaginary parts of the resonance line shape yields an estimate of

the plasma collision frequency. The measured and modeled resonance line shapes for a 50 kHz wave frequency are shown in Fig. 4. A plasma collision frequency of 110 ± 65 Hz was obtained for the $n = 1$ ion-cyclotron harmonics for a wave frequency range of 30–80 kHz. The low signal-to-noise in the line shape of the $n = 2$ ion-cyclotron resonance excluded any model fit.

The plasma collision frequency that results from the resonance line shape fits is almost 2 orders of magnitude smaller than that determined independently by our previous measurements of the ion response perpendicular to the axial B field [12] as well as from the measurement of Fokker-Planck diffusion coefficient [15]. As the width of the resonance pattern scales as $(\nu/\omega)^{1/3}$, the expected width should be ~ 5 times larger than the observed.

One possible hypothesis to explain the observed discrepancy between the resonance width and the obtained plasma collision frequency is to use a nonlinear model of particle trapping in the wave potential [1]. The calculated resonance trapping width [1] is given by $W_l = 4|e\Phi_0 J_l(k_\perp \rho)/M|^{1/2}$. The wave potential Φ_0 and $k_\perp \rho$ were determined by LIF [12] as 0.25 ± 0.02 and 0.025 ± 0.01 V, respectively. The trapping width of the $n = 1$ resonance is $(3.4 \pm 0.6) \times 10^4$ cm/s or $(0.85 \pm 0.15) \times v_{th||}$ which is in good agreement with the measured resonance line shape shown in Fig. 4. The estimated ion bounce frequency following Eq. (15) in Ref. [1] is $\approx 11.0 \pm 1.0$ kHz. Therefore, the trapped particles may encounter about a single bounce during the propagation of the wave along ≈ 10 cm from the antenna center, where the wave-particle resonance is observed. The limited amount of particle bounces in the wave potential trap as well as the relatively long coherence time is consistent with the validity of the linear theory of a weakly collisional plasma model. Nevertheless, the observed resonance width is

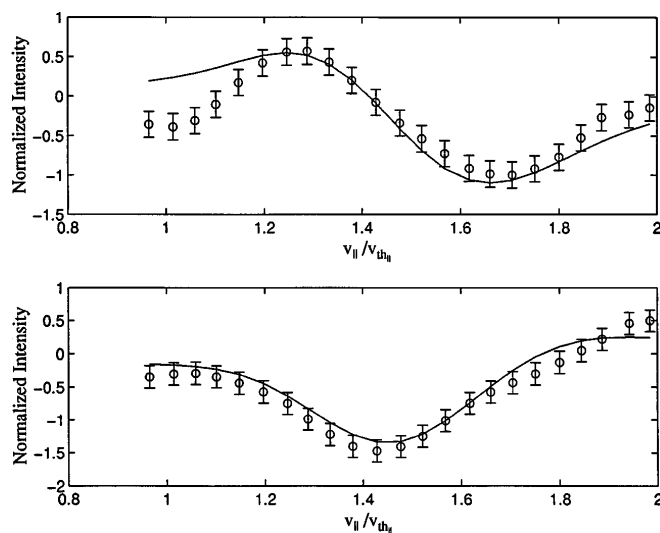


FIG. 4. The real (upper) and imaginary (lower) parts of the measured (circles) and modeled (solid) resonance line shapes of the first 50 kHz ion-cyclotron harmonic.

comparable to the nonlinear trapping width predicted by the wave-particle interaction model. Unfortunately, it is difficult experimentally to test the square-root scaling of the resonance width with wave potential. The resonance line vanishes at low wave amplitudes, partly due to low signal-to-noise ratio, and the small-amplitude assumption of the particle trapping model is unsatisfied in the case of large wave amplitudes.

In this Letter, the linear ion response to electrostatic ion-cyclotron waves parallel to the B field is measured in a weakly collisional plasma. The resonance lines of the $n = 1, 2$ harmonics are observed in the velocity resolved linear ion response to the waves. The velocity-space position of the wave-particle resonance satisfies the resonance condition over the measured wave frequency range. The shape of the first ion-cyclotron resonance line is modeled by a self-consistent 1D Poisson-Fokker-Planck equation in the limit of weak collisions. In principle, the best fit of the model to the measured resonance line shape should yield the plasma collision frequency for the velocity group of ions that resonate with the waves. However, the collision frequency determined from the resonance line fit is inconsistent with our previous independent measurements [12,15]. A future study is needed to resolve this discrepancy. The agreement of the calculated trapping width with the observed one may suggest that nonlinear effects contribute to the measured resonance line shape.

This research is supported by the National Science Foundation Grant No. PHY-9224548.

-
- [1] G.R. Smith and A.N. Kaufman, *Phys. Fluids* **21**, 2230 (1978).
 - [2] N.G. Van Kampen, *Physica (Utrecht)* **21**, 949 (1955).
 - [3] K.M. Case, *Ann. Phys. (N.Y.)* **7**, 349 (1959).
 - [4] R.A. Stern and J.A. Johnson, *Phys. Rev. Lett.* **34**, 1548 (1975).
 - [5] H. Ikezi and R.J. Taylor, *Phys. Rev. Lett.* **22**, 923 (1969).
 - [6] D. Gresillon, *Le Journal De Physique*, tome **32**, 269 (1971).
 - [7] S.A. Andersen, G.B. Christoffersen, V.O. Michelsen, and P. Nielsen, *Phys. Fluids* **14**, 990 (1971).
 - [8] R.A. Stern, D.L. Correll, H. Bohmer, and N. Rynn, *Phys. Rev. Lett.* **37**, 833 (1976).
 - [9] F. Skiff and F. Andereg, *Phys. Rev. Lett.* **59**, 896 (1987).
 - [10] F. Skiff, *Phys. IEEE Trans. Plasma Sci.* **20**, 701 (1992).
 - [11] A. Fasoli, T.N. Good, F. Andereg, F. Skiff, P.J. Paris, M.Q. Tran, and M. Yamada, *Phys. Rev. Lett.* **63**, 2052 (1989).
 - [12] M. Sarfaty, S. De Souza-Machado, and F. Skiff, *Phys. Plasmas* **3**, 1 (1996).
 - [13] A. Lenard and I.B. Bernstein, *Phys. Rev.* **112**, 1546 (1958).
 - [14] T.H. Stix, *The Theory of Plasma Waves* (American Institute of Physics, New York, 1992), pp. 247–262, 317–327.
 - [15] J.J. Curry, F. Skiff, M. Sarfaty, and T.N. Good, *Phys. Rev. Lett.* **74**, 1767 (1995).